



A Green Method of Reducing Graphene Oxide by Tangerine Peel Extract

RAGHAD ALI HAMID^{1,2} and RUZNIZA MOHD ZAWAWI^{1,*}

¹Department of Chemistry, Faculty of Science, Universiti Putra Malaysia, 43400 UPM Serdang, Selangor, Malaysia

²Department of Chemistry, College of Education for Pure Science, University of Kirkuk, Kirkuk 36001, Iraq

*Corresponding author: Tel: +60 3 97691445; E-mail: ruzniza@upm.edu.my

Received: 8 December 2023;

Accepted: 15 January 2024;

Published online: 31 January 2024;

AJC-21535

This work introduces a simple and environmental friendly approach for synthesizing reduced graphene oxide using tangerine peel extract as a non-toxic alternative to toxic compounds. Various microscopic and spectroscopic techniques were used to characterize the synthesized reduced graphene oxide. The UV-visible spectra of reduced graphene oxide (287 nm) at specific wavelengths and the FTIR analysis showed that the oxygen groups in reduced graphene oxide were reduced. Raman analysis confirmed a small increase in the intensity ratio of the D-band to the G-band. The X-ray diffraction spectra showed the presence of reduced graphene oxide in the 2 θ angle, at 28.36° peak with a d-spacing value of 2.12 nm. The wettability and morphology of reduced graphene oxide were also investigated. The carbon-to-oxygen ratio of reduced graphene oxide was increased compared to graphene oxide in addition, the cyclic voltammetry was used to evaluate the electrochemical behaviour of the reduced graphene oxide.

Keywords: Graphene oxide, Tangerine peel, Reduced graphene oxide, Green synthesis.

INTRODUCTION

Reduced graphene oxide (rGO) exhibits the exceptional chemical and physical properties, including high carrier mobility, larger surface area and optical transparency. Due to these properties, rGO is considered a popular composite material that can be used in various fields such as battery manufacturing and seawater desalination [1]. As a result, the development of novel techniques to produce graphene on a large scale has become a popular research area that attracts considerable attention. Although various techniques have been investigated, the graphene oxide (GO) reduction process is considered to be the most economical and reliable method [2]. Graphene is produced by a variety of processes, including chemical vapour deposition, electrochemical exfoliation and mechanical exfoliation [3].

Although the chemical reduction method of reducing GO to produce rGO offers significant advantages [4], it requires the use of potentially harmful toxic substances, such as sodium borohydride, sodium hydroxide and hydrazine hydrate, *etc.* [5] demands for studies on alternative environmentally friendly reducing agents and environmentally friendly rGO production methods. Therefore, numerous studies have found that other green reducing compounds such as *Clinacanthus nutans*, glucose,

coconut, Indian gooseberry, onion juice, peppermint leaf extract, wild carrot root, vitamin C, sugarcane bagasse extract, tea solutions, sodium bisulfite and dried marigold flowers are viable, environmentally safe reducing compounds that readily react with oxygen in the functional group of GO [6]. If the method for synthesis of plant extracts can be optimized, they would be a renewable and cost-effective compound for the reduction of GO to produce rGO, potentially providing similar or better reduction rates than conventional hydrazine [7].

Tangerine peel or *Citrus reticulata pericardium* is the epidermal layer of various varieties of oranges that have been dehydrated. According to Chinese custom, tangerine peel is used to treat bronchial asthma, dyspepsia and cardiovascular diseases, among others [8]. It contains a variety of active ingredients, including polysaccharides, alkaloids, flavonoids, essential oils and vitamins; tangerine peel is considered a potential ingredient for health foods. Of these active compounds, flavonoids are considered the most important. Pharmacological studies show that flavonoids contained in tangerine peel have anticancer, anticoagulant, antiplatelet, anti-anaphylactic, antioxidant and antiviral properties. The extraction of flavonoids from tangerine peel could be supported by sustainable development and a circular economy to produce high-quality products [9].

To the best of our knowledge, the present study is the first to investigate the use of tangerine peel as a reducing agent for the preparation of rGO. A literature search revealed that a reducing compound should have an excellent reducing capacity without the need for additional purification or separation of a particular species. Therefore, the present study identified an environmentally friendly, efficient and cost-effective method for using tangerine peel extract for the chemical reduction of graphene oxide. The microscopic and spectroscopic studies such as UV-Vis spectroscopy, X-ray diffraction (XRD), wettability properties, Fourier transform infrared (FTIR) spectroscopy, Raman spectroscopy and scanning electron microscopy (SEM) were used to characterize the reduction of GO to rGO. The cyclic voltammetry (CV) was also used to evaluate the synthesized rGO and demonstrate its effectiveness in various electrochemical applications. The present approach has many advantages, such as environmental friendly reducing agent, easy production of the extract and non-toxic waste generated at the end of the reduction process.

EXPERIMENTAL

In this study, 99.9% graphene oxide (GO) powder was purchased from Sigma-Aldrich, USA, while potassium hexacyanoferrate (III), ethyl alcohol (95% (v/v) and potassium chloride were procured from ChemiZ (M) Sdn. Bhd., Malaysia. The deionized water with a purification of 18.2 M Ω cm was obtained from Millipore purification system.

Preparation of tangerine peel extract: Tangerine fruit was obtained from the local fruit store in Malaysia. The peels were separated from the fruit and first rinsed under running water before being rinsed a second time with deionized water and dried in an oven at 50 °C. A household blender was then used to grind the dried peels into a dried peel powder and stored in an airtight container. To prepare the peel extract, dried peel powder (6 g) was suspended in deionized water (150 mL) and heated to boiling at 80 °C for 30 min. The mixture was then filtered and stored at 5 °C for later use.

Synthesis of reduced graphene oxide (rGO): Tangerine peel extract was used to synthesize rGO from GO precursors. For this purpose, deionized water (60 mL) was added to GO

powder (40 mg) before sonication of the mixture for 1.5 h. The mixture was then mixed with water and then treated with tangerine peel extract (30 mL) and finally heated to 90 °C in a waterbath for 2 h with constant stirring. To determine the ideal temperature, the thermal reactions were studied at different temperatures. Table-1 shows the different temperatures used in the experiment (50, 80 and 90 °C). The time and concentration of the peel extract were kept constant throughout the experiment. Following the reaction, after cooling to room temperature, the mixture was centrifuged at 3000 rpm for 60 min to remove any remaining impurities. The pellet was then rinsed several times with deionized water. The data from the UV-Vis spectrum were utilized in the subsequent optimization studies. The concentration of the peel extracts and the reaction time were optimized, while the other parameters were kept constant. Finally, the black precipitate that formed was collected and dried in an oven at 80 °C for 2 h. The change in colour from brownish green to black indicates GO deoxygenation. Fig. 1 shows the reaction involved during the chemical reduction of GO with tangerine peel extracts. Graphene oxide contains functional groups such as epoxy (C-O-C) and hydroxyl groups (OH) at its periphery. The epoxy groups become ring-opening upon reaction with the polyhydroxy functional groups of tangerine extract compound. Reduction of GO occurs as a result of deoxygenation brought about by condensation, which involves the loss of water molecules and further rearrangement results in the stretching the loop.

TABLE-1
OPTIMIZED PARAMETER VARIABLES FOR rGO SYNTHESIS

Parameter	Variable values
Time	1, 1.5 and 2 h
Temperature	50, 80, 90 °C
Peel extract concentration	10, 20, 30 (v/v) %

UV-visible analysis: Electronic absorption spectra were measured at a wavelength range from 200 to 800 nm at room temperature and atmospheric pressure using a Shimadzu UV-1650PC UV-visible reflective spectrophotometer (Japan).

X-ray diffraction (XRD) analysis: A Shimadzu XRD-6000 X-ray diffractometer (Japan) was used to determine the crystallinity using a CuK α radiation ($\lambda = 0.15406$ nm), 2 θ

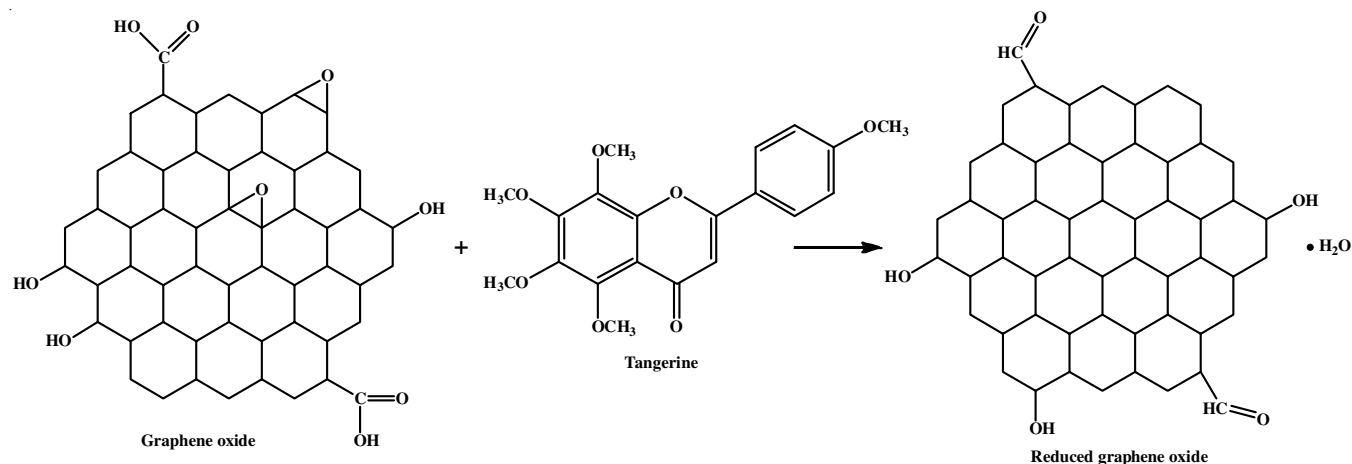


Fig. 1. The reaction of chemical reduction of graphene oxide (GO) by tangerine peel extract

between 20 and 80° at 30 kV, 15 mA and a scan speed of 2° min⁻¹. X'Pert Highscore XRD analysis software and a JCPDS standard file was used to further analyze the diffractograms.

Raman analysis: A Raman imaging microscope from WITec (Germany) with a 488 nm wavelength laser was used to analyze the samples GO and rGO to gain new insights into characterizing the different aspects of the microstructures of these materials. A laser beam with an excitation power of 20 mW, an excitation wavelength of 532 nm, an exposure time of 20 s, a spectral range of 4000-500 cm⁻¹ was used to determine the Raman spectra.

FTIR analysis: A Perkin-Elmer 1600 FTIR spectrophotometer (USA) was used to measure the infrared spectra of samples in the wavelength range 4000-500 cm⁻¹ on polyaniline (PANI) pellets prepared with potassium bromide.

SEM analysis: A JOEL JSM-6400 SEM (Japan), equipped with an in-lens detector, was used to analyze the thickness of GO and rGO and to determine the morphological characteristics of the GO particles and rGO.

Contact angle: A POWEREACH JC200D2 (country) iattention theta lite optical tensiometer and stress image analysis software were used to measure the surface hydrophobicity of each film. The analysis was performed at room temperature (25 ± 2 °C) using the sessile drop method. The sample was applied to a glass slide and allowed to dry before a drop of deionized water (3 µL) was added to the surface of each film and the angle formed at the liquid-solid and liquid-vapour (θ) interfaces was measured as contact angle.

Electrochemical studies: Metrohm Multi-Autolab M101 and Nova software 2.1.4 (Netherlands) were used to perform the electrochemical experiments. A cyclic voltammetric (CV) analysis was performed using electroanalytical measurement software on a computer. In this study, a platinum wire and a silver/silver chloride electrode (Ag/AgCl) were used as counter and reference electrodes, respectively, while a glassy carbon electrode (GCE) with a diameter of 3 mm was used as working electrode. The GCE was prepared by manually polished with alumina pastes with different particle sizes of 0.05 µm. The electrode was then rinsed with ultrapure water using Millipore's Milli-Q system and sonicated for 15 min. The GCE was modified with GO and rGO by applying a prepared suspension of GO 10 µL of 0.28 mg mL⁻¹ GO, suspended in 0.2 mol L⁻¹ sodium sulfate solution, to the GCE surface to dry and form a film at room temperature for at least 5 h. For all voltammetric measurements, a 0.1 M KCl solution containing 1 mM potassium ferricyanide was used at a scan rate of 100 mV s⁻¹ unless otherwise specified. Solutions were degassed with nitrogen for 8 min before recording voltammograms. Samples were scanned in the potential range of -0.4 V to 0.6 V.

RESULTS AND DISCUSSION

The reduction of graphene oxide (GO) to reduced graphene oxide (rGO) was studied by UV-Vis spectroscopic analysis. This observation represents the degree of reduction of the graphene oxide. The UV-Vis absorption spectra of GO and rGO are shown in Fig. 2a. The absorption peak at 250 nm in the spectrum of GO was attributed to the π - π^* transitions of the aromatic C=C

bonds. Since the absorption peak was red-shifted after reduction to 287 nm, this indicates the reactivation of the conjugated C=C bonds. The shift of the absorption peak from 250 to 287 nm indicates the removal of oxygen containing functional groups by the tangerine peel extract [10]. Fig. 2b shows that the maximum rGO absorbance was observed at 214 nm at a concentration of 10% tangerine peel extract. This absorbance was higher than that at concentrations of 20% and 30%, which was determined at 217 and 219 nm, respectively. The absorbance of rGO increased with increasing concentration of tangerine peel extract to confirm the effectiveness of the activity with tangerine peel extract in eliminating the oxygenated groups and to demonstrate its decrease, leading to the higher absorbance [11].

Fig. 2c shows the absorption spectra of rGO for the effect of temperatures (50, 80 and 90 °C) at different wavelengths (280, 281 and 284 nm). The absorption peaks were higher at 90 °C than at the other temperatures [12]. At a high temperature of 90 °C, decomposition of oxygen containing groups occurs by removal of large oxygen containing clusters. Fig. 2d shows the absorption spectra of rGO at reaction times of 1, 1.5 and 2 h. The absorption peak gradually increased as the time was increased from 1 to 2 h. When the reaction time was increased to 2 h, the maximum absorbance peak shifted to 287 nm, indicating that rGO was fully formed. The intense peak at 287 nm, which is the main product formed by the sp^2 lattice recovered from graphene [13].

XRD studies: The changes in graphene crystal structure were studied before and after reduction with tangerine peel extracts [14]. The XRD patterns of GO and rGO are shown in Fig. 3. The diffraction peaks for GO are observed at 26.45° and 42.95° and the calculated d-spacing for GO was found to be 3.39 nm [15]. The presence of a broad peak at 28.36° for rGO indicates that the crystal phase (002) is randomly arranged compared to the highly crystallized structure of GO. The rGO diffraction peak shifted from 26° to 28° and the d-spacing decreased to 2.12 nm. The elimination of the oxygen containing functional groups between the different graphite layers leads to a decrease in the d-spacing. Another less intense rGO peak is observed at 43.02° with (001) orientation, which is due to the turbostratic band of disordered carbon material. This indicates the evolution of well-ordered and low-stratified graphene. The spacing between graphene layers was comparable to that of graphite [16].

FTIR studies: A broad peak at 3616 and 3610 cm⁻¹ was attributed to the O-H stretching vibrations before and after the interactions between GO and the tangerine peel extract (Fig. 4). The asymmetric and symmetric CH₂ stretching of GO is responsible for the IR peaks that correspond to 2577 cm⁻¹ and 2194 cm⁻¹. There were no obvious stretching vibration peaks in the spectra of rGO after the reaction, suggesting that the tangerine peel extract reduces the C-O bond in GO [17]. The peak at 1978 cm⁻¹ before the reaction indicated the presence of the C=O vibration of the COOH group of the carboxylic acid in GO. The stretching vibration peaks of C-O (epoxy) at 1240 cm⁻¹ and C-O (alkoxy) at 925 cm⁻¹ observed a significant decrease, respectively. The use of tangerine peel extract signifi-

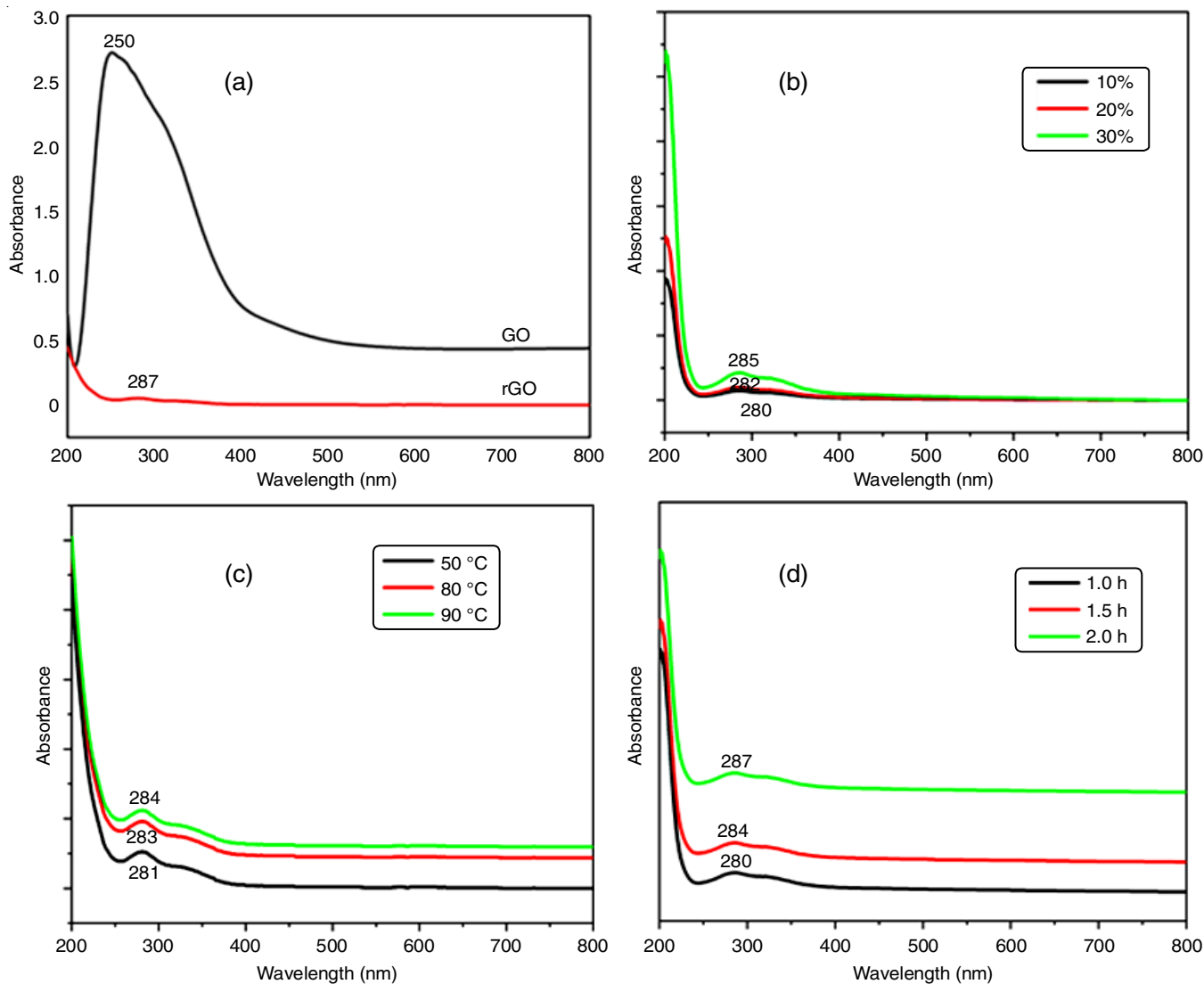


Fig. 2. Absorption spectrum of rGO from 200 to 800 nm in the UV-visible range at (a) GO and rGO, (b) different concentrations of tangerine peel, (c) temperature dependence of rGO, (d) time dependence of GO reduction

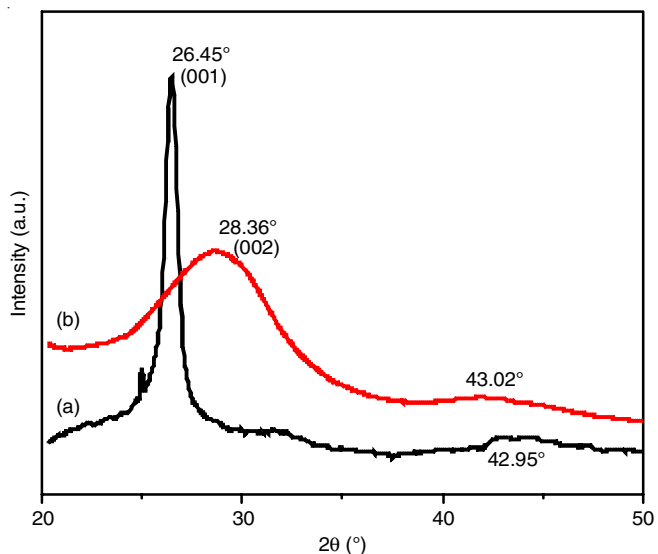


Fig. 3. X-ray diffraction (XRD) pattern of (a) GO, (b) rGO by tangerine peels extract

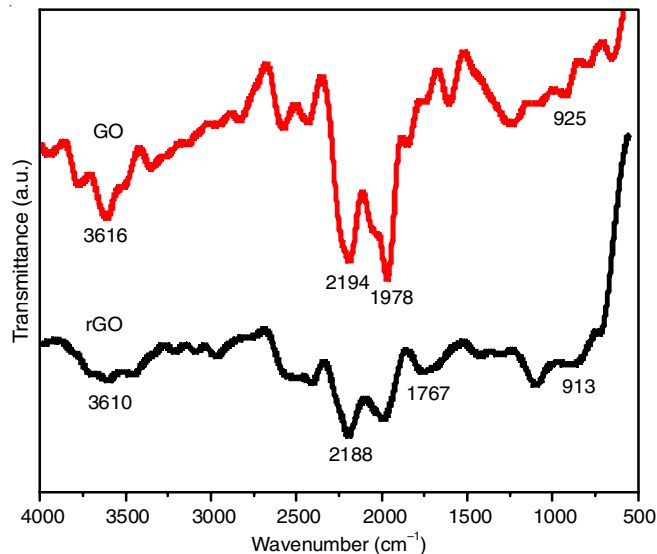


Fig. 4. FT-IR spectra of (a) graphene oxide (GO) and (b) reduction of graphene oxide (rGO)

cantly reduced the intensity of the O-H and C-O bands of the rGO samples after the reaction. The carbon-to-oxygen (C/O) ratio of the samples was also quantitatively analyzed [18]. It was also found that the peaks for O-H, C=O and C-O functional groups were significantly attenuated compared to those of the pure GO sample. Thus, both of these results and the UV-vis results accord well [19] indicated that GO had been reduced to rGO.

Raman studies: The graphene molecules on the substrate and in suspension exhibited similar Raman spectra [20]. The reference bulk graphite used for layer formation was measured. Due to the different electrical band structures of the multilayer graphene, numerous peaks were found in the 2D band of this material [21]. The Raman spectra of the rGO molecules reduced with tangerine peel extract showed two primary characteristics. The D band of rGO was found at 1568 and 2707 cm^{-1} , while the G band was found at 1351 cm^{-1} . On the other hand, the D band of GO at 1343 cm^{-1} (D-band) and 1563 and 2698 cm^{-1} for the G-band show (Fig. 5) defect-induced band corresponds to structural defects and disorder, while the G-band is associated with the in-phase vibration of the sp^2 carbon network of the graphitic domain [22]. The high ID:IG ratio of 0.85 for GO indicates that the graphitic planes are functionalized with

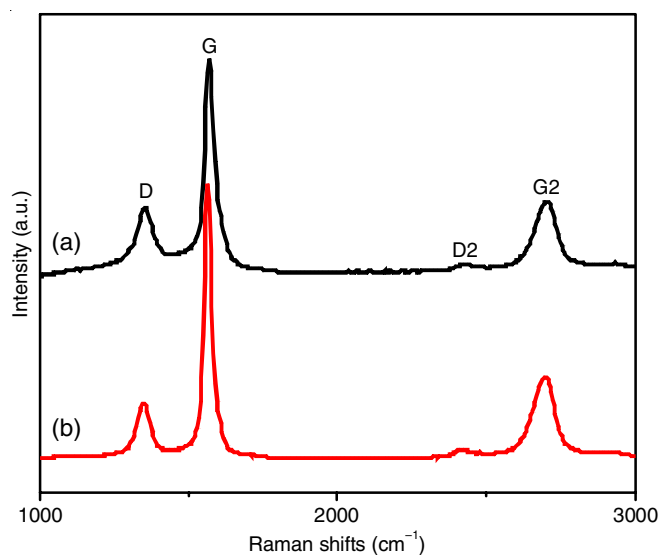


Fig. 5. Raman spectra of (a) GO and (b) rGO

oxygen. The preparation of composites and subsequent reduction of GO can be determined from the lower wavenumber G-band, indicating an increase in sp^2 carbon atoms. Moreover, the decrease of the ID:IG ratio to 1.16 indicates the loss of oxygen functionality. This implies that graphene oxide and reduced graphene oxide have a multilayer structure. The results also show that the 2D band shifts to a higher value after the reduction of GO indicating that the graphene layer is stacked. Since GO contains various functional groups, they could prevent the stacking of the graphene layer [23].

Wettability of GO: It is necessary to thoroughly understand the behaviour of graphene on surfaces, especially the wetting behaviour, to determine the wide-ranging applications of the material. Although graphene cannot be easily classified as hydrophobic or hydrophilic due to its 2D structure, it leads to a variety of interfacial processes that control its apparent wettability [24]. It is crucial to investigate the wettability of graphene, as graphene with hydrophobic properties can limit the deposition of liquids and reduce contamination in the manufacture of electrical devices [25].

As observed in Fig. 6, the GO membrane had a contact angle with acetone 21.4°, indicating that this GO membrane is hydrophilic. The presence of several oxygen functional groups on the surface of GO membrane is responsible for its hydrophilicity. The rGO membrane had a contact angle of 96.7° indicating that the reduction reaction increased the hydrophobicity of the membrane because fewer oxygen functional groups were present on the surface of GO. This increased the surface hydrophobicity of the GO film, which may be attributed to the reduction of GO using tangerine peel extract.

Morphological studies: The morphology of GO and rGO was analyzed by scanning electron microscopy (SEM) and the results are shown in Fig. 7, which show the appearance of wrinkles and folded areas with the corrugated morphology. Comparison of the corrugated morphology and the images of the folded domains GO, SEM images show that the corrugated structure of rGO with some closely stacked individual layers is due to the new functional groups formed by the reduction with the tangerine peel extract [26]. The oxygenated functional groups were eliminated at the basal planes and edges of the GO sheets ensuring that the graphene sheets could interact closely with each other and build up *via* strong π - π^* stacking

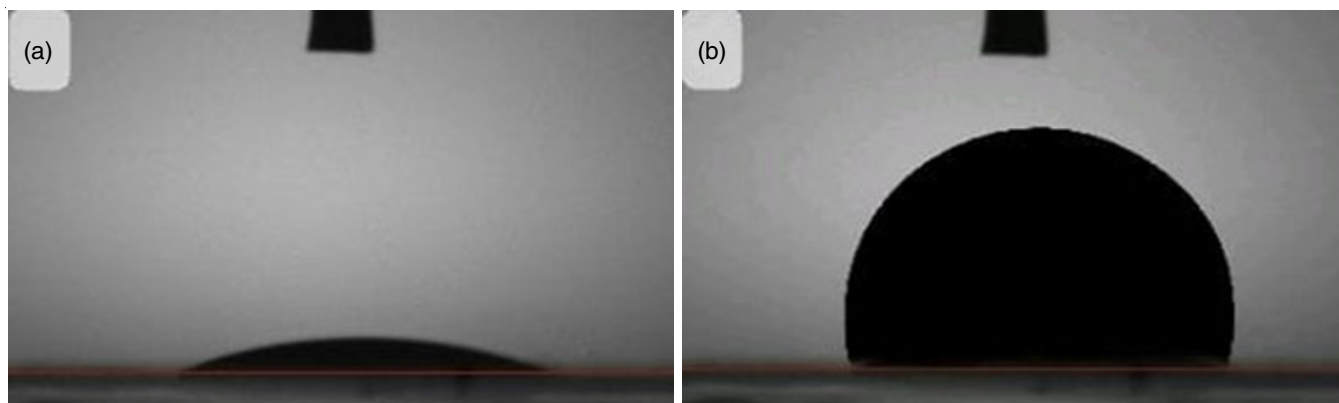


Fig. 6. Contact angle of (a) GO and (b) rGO

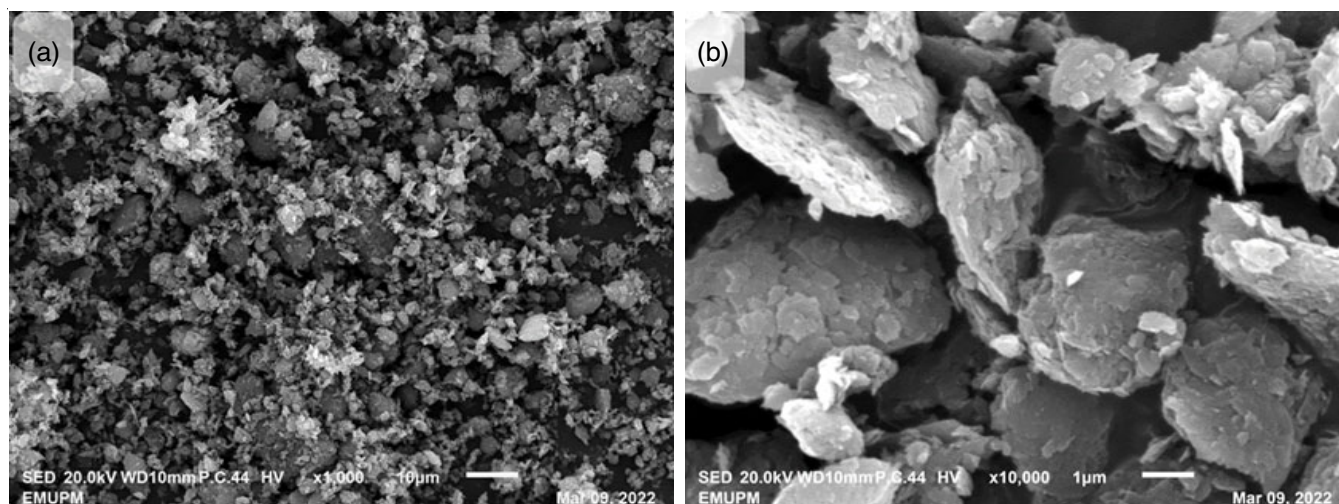


Fig. 7. SEM images of (a) GO and (b) rGO

and van der Waals forces. This conclusion is consistent with the results of XRD studies indicating that the interlayer spacing of rGO is smaller than that of GO, which improves the stacking of rGO sheets. However, some wrinkles were still present on the surface of rGO, which might be due to the biomolecules of tangerine peel extract loaded on the surface of rGO during the reduction process [27].

Electrochemical behaviour: Cyclic voltammetry (CV) was used to investigate the electrochemical behaviour of the rGO-modified electrode. Fig. 8a shows the CVs of bare, GO- and rGO-modified GCE recorded in 0.1 M KCl with 1 mM $K_3Fe(CN)_6$ solution at a scanning rate of 100 mV s^{-1} . The current responses for the electrodes in ascending order are as follows: bare GCE < GO/GCE < rGO/GCE. A pair of low redox peak currents with a peak separation (ΔE_p) of 0.23 V was visible at bare GCE indicating that electron transport at the surface is slow. This current increases for the graphene-based modified electrodes. The rGO/GCE shows the highest oxidation peak current of $19\ \mu\text{A}$ with ΔE_p of 0.112 V [28]. This peak current increase in rGO is due to the restoration of sp^2 structure in rGO after the reduction of graphene oxide reduced the defects and sp^3 structure of carbon–oxygen, which hinders the electron transport within the structure. The peak separation of rGO/

GCE is also reduced due to the electrokinetic behaviour of the electrode, which improves the electroactive surface area and conductivity [29].

The effect of peak current on rGO/GCE was also investigated at different scan rates, as shown in Fig. 8b-c. As expected, the redox peak currents increased at higher scan rates and the anodic (I_{pa}) and cathodic (I_{pc}) peak currents are linearly dependent on the square root of the scan rate in the range of 10 to 100 mV s^{-1} with a linear regression, R^2 of 0.991 and 0.997, respectively. These results indicate that the electrochemical behaviour is controlled by the diffusion process, as the contribution of diffusion plays an important role in the electrode response, since the electron transfer process of ferricyanide is faster at the rGO/GCE-modified electrode [30].

For a diffusion-controlled process, the Randles–Sevcik equation is used to calculate the electroactive surface area of the electrode [31].

$$I_p = (2.69 \times 10^5) A \times D^{1/2} \times n^{2/3} \times C \times v^{1/2} \quad (1)$$

where I_p = peak current, n = number of electrons transferred; A = active surface area; D = diffusion coefficient for $K_3[Fe(CN)_6]$ ($7.6 \times 10^{-6}\text{ cm}^2\text{ s}^{-1}$) [32]; C = analyte concentration (mL); and v = scan rate (mV/s).

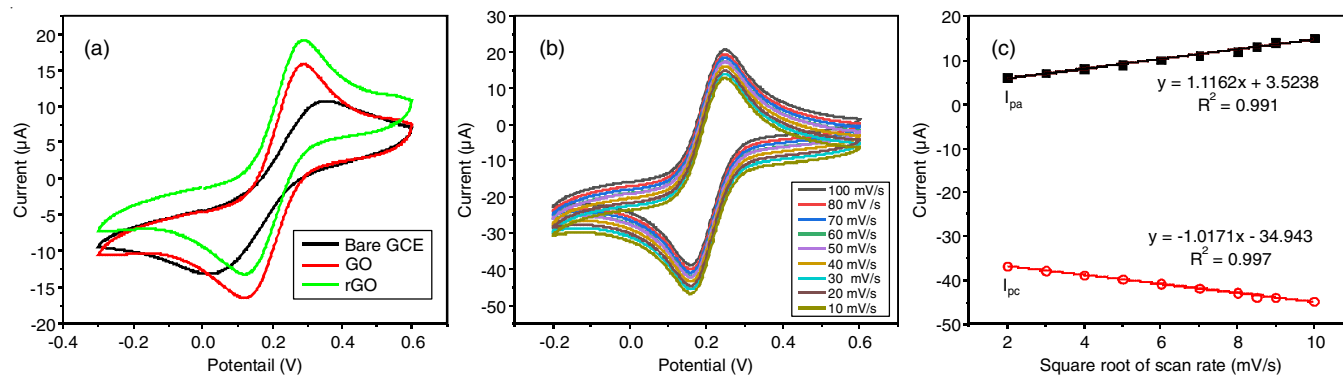


Fig. 8. Cyclic voltammograms (CV) were obtained for (a) bare GCE, GO-GCE and rGO-GCE in a 0.1 M KCl solution containing 1 mM $K_3Fe(CN)_6$, using a scan rate of 100 mV s^{-1} ; (b) cyclic voltammograms of rGO/GCE at different scan rates (10– 100 mV s^{-1}) in 0.1 M KCl solution containing 1 mM $K_3Fe(CN)_6$ and (c) Plot of anodic and cathodic peak current (I_p) vs. square root of scan rate ($V^{1/2}$)

The active surface area of rGO/GCE was 0.024 cm², which was larger than that of bare GCE 0.016 cm². The results of CV analysis was also excellent under the identical conditions. Therefore, rGO is a potential compound in the electrochemical field due to its unique properties and potential applications in drug delivery, catalysis, sensing, solar cells and field effect transistors (FET) [33].

Conclusion

The present study demonstrated that tangerine peel extract can effectively and successfully reduce graphene oxide within 2 h. A variety of spectroscopic and microscopic methods such as XRD, UV-Vis and Raman spectroscopies were used to characterize the synthesized rGO. In addition, this reduction method was used to demonstrate the nature of surface after increasing the contact angle and indicated that rGO is hydrophobic as confirmed from the wettability test. The results of SEM and FTIR showed that the C/O ratio was low in the GO structures but played a greater role in the rGO structures with reduced number of oxygen. Moreover, the rGO-modified GCEs exhibited the highest peak current demonstrating their electrochemical activity as determined *via* cyclic voltammetry. This study emphasizes the significance of minimizing the use of potentially harmful chemicals in the synthesis process, in addition to meet the demand for graphene derivatives.

ACKNOWLEDGEMENTS

The authors thank Ministry of Higher Education Malaysia for funding this study under Grant no.: FRGS/1/2020/STG04/UPM/02/7. Special thanks to Department of Chemistry, Faculty of Science Institute of Nanoscience and Nanotechnology and Institute of Bioscience, University Putra Malaysia for the research facilities provided.

CONFLICT OF INTEREST

The authors declare that there is no conflict of interests regarding the publication of this article.

REFERENCES

- F. Maeda and H. Hibino, *Diamond Related Materials*, **34**, 84 (2013); <https://doi.org/10.1016/j.diamond.2013.02.007>
- M. Cossutta, J. McKechnie and S.J. Pickering, *Green Chem.*, **17**, 5874 (2017); <https://doi.org/10.1039/C7GC02444D>
- G.B. Mahendran, S.J. Ramalingam, J. Rayappan, S. Kesavan, T. Periatthambi and N. Nesakumar, *J. Mater. Sci. Mater. Electron.*, **31**, 14345 (2020); <https://doi.org/10.1007/s10854-020-03994-4>
- S. Thakur and N. Karak, *Carbon*, **50**, 5331 (2012); <https://doi.org/10.1016/j.carbon.2012.07.023>
- M.Z. Ansari, R. Johari and W.A. Siddiqi, *Mater. Res. Express*, **6**, 055027 (2019); <https://doi.org/10.1088/2053-1591/ab0439>
- D. Perumal, E. Albert, N. Saad, T. Hin, R.M. Zawawi, H. Teh and C.C. Abdullah, *Crystals*, **11**, 1539 (2022); <https://doi.org/10.3390/cryst12111539>
- K.K.H. De Silva, H.-H. Huang, R.K. Joshi and M. Yoshimura, *Carbon*, **119**, 190 (2017); <https://doi.org/10.1016/j.carbon.2017.04.025>
- Q. He and K. Xiao, *Food Control*, **69**, 339 (2016); <https://doi.org/10.1016/j.foodcont.2016.05.019>
- B. Haghighi, and, M.A. Tabrizi, *RSC Adv.*, **32**, 13365 (2013); <https://doi.org/10.1039/C3RA40856F>
- P.C. Nethravathi, G.S. Shruthi, Udayabhanu, H. Nagabhushana, D. Suresh and S.C. Sharma, *Ceram. Int.*, **41**, 8680 (2015); <https://doi.org/10.1016/j.ceramint.2015.03.084>
- S. Mahata, A. Sahu, P. Shukla, A. Rai, M. Singh and V.K. Rai, *New J. Chem.*, **42**, 19945 (2018); <https://doi.org/10.1039/C8NJ04086A>
- A. Baioun, H. Kellawi and A. Falah, *Carbon Lett.*, **24**, 47 (2017); <https://doi.org/10.5714/CL.2017.24.047>
- X. Jin, N. Li, X. Weng, C. Li and Z. Chen, *Chemosphere*, **208**, 417 (2018); <https://doi.org/10.1016/j.chemosphere.2018.05.199>
- M.S.A. Faiz, C.A.C. Azurahaman, S.A. Raba'ah and M.Z. Ruzniza, *Results Phys.*, **16**, 102954 (2020); <https://doi.org/10.1016/j.rinp.2020.102954>
- D.R. Madhuri, K. Kavyashree, A.R. Lamani, H.S. Jayanna, G. Nagaraju and S. Mundinamani, *Mater. Today Proc.*, **49**, 865 (2022); <https://doi.org/10.1016/j.matpr.2021.06.173>
- A. Razaq, F. Bibi, X. Zheng, R. Papadakis, S.H.M. Jafri and H. Li, *Materials*, **15**, 1012 (2022); <https://doi.org/10.3390/ma15031012>
- O. Moradi and S. Panahandeh, *Environ. Res.*, **214**, 114042 (2022); <https://doi.org/10.1016/j.envres.2022.114042>
- Q. Xu, X. Lin, L. Gan, G. Owens and Z. Chen, *J. Colloid Interface Sci.*, **605**, 881 (2022); <https://doi.org/10.1016/j.jcis.2021.07.102>
- S. Shamailla, A.K.L. Sajjad, Quart-ul-Ain, S. Shaheen, A. Iqbal, S. Noor, G. Sughra and U. Ali, *J. Environ. Chem. Eng.*, **5**, 5770 (2017); <https://doi.org/10.1016/j.jece.2017.11.009>
- W. Liu, Z. Wang, W. Yan, Z. Zhao, L. Shi, L. Huang, Y. Liu, X. He and S. Cui, *Carbon*, **202**, 389 (2023); <https://doi.org/10.1016/j.carbon.2022.11.001>
- L.G. Cançado, A. Reina, J. Kong and M.S. Dresselhaus, *Phys. Rev. B*, **77**, 245408 (2008); <https://doi.org/10.1103/PhysRevB.77.245408>
- M. Mahiuddin and B. Ochiai, *Mater. Today Sustain.*, **22**, 100383 (2023); <https://doi.org/10.1016/j.mtsust.2023.100383>
- P. Rajapaksha, R. Orrell-Trigg, D. Shah, S. Cheeseman, K.B. Vu, S.T. Ngo, B.J. Murdoch, N.R. Choudhury, H. Yin, D. Cozzolino, Y.B. Truong, A.F. Lee, V.K. Truong and J. Chapman, *Mater. Today Chem.*, **27**, 101242 (2023); <https://doi.org/10.1016/j.mtchem.2022.101242>
- L.A. Belyaeva and G.F. Schneider, *Surf. Sci. Rep.*, **75**, 100482 (2020); <https://doi.org/10.1016/j.surfrep.2020.100482>
- J. Feng and Z. Guo, *Nanoscale Horiz.*, **4**, 339 (2019); <https://doi.org/10.1039/C8NH00348C>
- B. Li, X. Jin, J. Lin and Z. Chen, *J. Clean. Prod.*, **189**, 128 (2018); <https://doi.org/10.1016/j.jclepro.2018.04.018>
- S. Nasir, M.Z. Hussein, N.A. Yusof and Z. Zainal, *Nanomaterials*, **7**, 182 (2017); <https://doi.org/10.3390/nano7070182>
- N.A. Edris, J. Abdullah, S. Kamaruzaman, M.I. Saiman and Y. Sulaiman, *Arab. J. Chem.*, **11**, 1301 (2018); <https://doi.org/10.1016/j.arabjc.2018.09.002>
- N.I.A.M. Mokhtar, S.E. Ashari and R.M. Zawawi, *RSC Adv.*, **13**, 13493 (2023); <https://doi.org/10.1039/D3RA01060K>
- L. Shahriary and A.A. Athawale, *Energy Environ. Eng.*, **2**, 58 (2014).
- M.J. Song, S.W. Hwang and D. Whang, *J. Appl. Electrochem.*, **10**, 2099 (2010); <https://doi.org/10.1007/s10800-010-0191-x>
- S.J. Konopka and B. McDuffie, *Anal. Chem.*, **42**, 1741 (1970); <https://doi.org/10.1021/ac50160a042>
- S. Yang, G. Li, N. Xia, Y. Wang, P. Liu and L. Qu, *J. Alloys Compd.*, **853**, 157077 (2021); <https://doi.org/10.1016/j.jallcom.2020.157077>